Correlation of Laminar Flame Speed with Lower Flammability Limit for Various Fuel-Air Mixtures

Submitted in partial fulfilment of the requirements for the degree of

PROFESSIONAL MASTER'S PROGRAM

in

CHEMICAL ENGINEERING

by

CHAITANYA KUMAR REDDY POCHA

Under the guidance of

Industry Mentors: Mr. Silvio Esterellas & Dr. Wang Zhiyan

Academic Mentors: Dr. Ray A. Mentzer & Dr. William R. Clark

Davidson School of Chemical Engineering
PURDUE UNIVERSITY
West Lafayette, U.S.A.

04 DECEMBER 2023

STATEMENT OF ORIGINAL AUTHORSHIP

I hereby declare that the project report titled 'Correlation of Laminar Flame Speed with Lower

Flammability Limit for Various Fuel-Air Mixtures' submitted by Chaitanya Kumar Reddy Pocha,

for the award of the degree of Professional Master's Program in Chemical Engineering to Purdue

University, is a record of work carried out by me under the supervision of academic mentors (Dr.

Ray Mentzer & Dr. William R. Clark) and industrial mentors (Mr. Silvio Esterellas & Dr. Wang

Zhiyan).

The work contained within this project report has not been previously submitted to meet the

requirements for an award at this or any other higher education institution. To the best of my

knowledge and belief, this report contains no material previously published or written by any other

person, except where due reference is made in the text of the thesis.

POCHA CHAITANYAKUMAR REDDY

DECEMBER 2023

ii

Table of Contents

1.	I	Introduction							
2.	Literature Review								
3.	F	Results	and discussion	6					
	3.1	Imp	pact of equivalence ratio on laminar flame speeds of various fuel and air mixtures	6					
	3	.1.1	Methane-air mixtures	6					
	3	.1.2	Hydrogen-air mixtures						
	3	.1.3	Ethane-air mixtures						
	3.1.4		Ethylene-air mixtures	9					
	3	.1.5	Propane-air mixtures	0					
	3.2	Fla	me speed calculations near LFL range1	1					
	3.3	Coı	ncentrations of fuel-air mixtures at set S _L values	3					
4.	(Conclu	sion	8					
5.	F	uture	steps1	9					
6.	F	Referen	nces	i					
7. Appendix									
	7.1	7.1 Flame Code function for calculating S _L							
	7.2	Co	de for returning S_L value at a particular T,P and X	vi					

1. INTRODUCTION

Combustion, a fundamental process in energy conversion and propulsion, involves the rapid chemical reaction between a fuel and oxidizer, releasing heat and producing products like water and carbon dioxide¹. Understanding combustion dynamics is crucial for optimizing efficiency and minimizing environmental impact in applications ranging from internal combustion engines to industrial furnaces. At the heart of combustion research lies the laminar flame speed (S_L), a key parameter representing the velocity of a stable, one-dimensional adiabatic flame². Laminar flame speed encapsulates critical details about reactivity, diffusivity, and the overall combustion process. This introductory exploration delves into the significance of laminar flame speed, unraveling its role in comprehending combustion phenomena and its broader implications for designing efficient and environmentally conscious energy systems^{3, 4}.

During this project, I have reviewed the experimental measurements of laminar flame speeds using a Bunsen burner flame of common fuel and air mixtures and compared them with the theoretical models in Python software. Some of the models employed in this project include the use of GRI30 Mech III model, which is built-in the Cantera Library, the H2O2 model, also built-in Cantera, and the USC Mech II model which is modelled by Combustion Laboratory at USC. These models use thermodynamic, transport and combustion reaction mechanisms to reach an estimate of the laminar flame speed for a particular fuel-air mixture. For the model to calculate the propagation speed, it needs (1) type of fuel, (2) composition of fuel-air mixture, specified in terms of molar fraction, (3) the temperature of the fuel, and (4) the pressure of the fuel. The program then gives an estimate of the flame speed which is used to produce a profile of flame speeds at different equivalence ratios for various fuels. Some of the common fuels include the C1-C5 hydrocarbons, hydrogen, and Ammonia. Since this project focuses on lower flammability limit (LFL), comparisons were made

at the equivalence ratios less than 1. A table is created to compare the experimental and theoretical flame speeds and their deviations for various fuel-air mixtures near the LFL range.

The second part of this project is focused on measuring the flame speeds, particularly at the LFL value. The NFPA 68 document was used to get the standard LFL values used in the US and the UK, which were usually in the units of vol% of fuel in air. Now, at the LFL value itself, the prediction is that the flame speed be exactly at 0 m/s. However, numerical models give a value that is higher than 0 because there is an experimental and theoretical discrepancy on what the actual LFL value is. Hence, using the GRI30, H2O2 and the USC Mech II models, LFL estimates were back calculated by using the Fsolve function in python, which basically calculates the composition of the fuel-air mixture at which the flame speed is 0 m/s. The discrepancies between the LFL values documented in NFPA 68 and the Cantera model are noted in a table. Furthermore, a correlation graph of model-predicted flame speed at the LFL is plotted against the LFL value itself. Based on this graph, concentrations of all different fuel-air mixtures are estimated at 2 cm/s and 4 cm/s flame speeds. Finally, a conclusion was reached on the minimum value for the laminar flame speed so that a flame is guaranteed for any fuel-air mixture.

2. LITERATURE REVIEW

Laminar flame speed stands as a linchpin in the realm of combustion, wielding influence over a spectrum of crucial domains. Its role in combustion efficiency is paramount, acting as the tempo conductor orchestrating the rapid dance between fuel and oxidizer. In internal combustion engines, the flame speed shapes the rhythm of energy release, directly impacting performance and efficiency^{4, 5}. Beyond the confines of engines, it plays a pivotal role in safety assessments, aiding in the design of preventative measures in industrial settings. Moreover, this parameter contributes to pollution control by influencing combustion rates and emission levels. Flame stability hinges

on laminar flame speed, determining the delicate balance between controlled burns and turbulent unpredictability⁶. In the world of fundamental research, it serves as a cornerstone, unraveling the complexities of combustion dynamics. Whether optimizing engines, ensuring safety, or unraveling the mysteries of combustion, laminar flame speed emerges as an indispensable player, setting the pace for a myriad of critical processes^{7, 8}.

In the domain of combustion research, scientists deploy a diverse array of methodologies to ascertain the elusive laminar flame speed. Foremost among these is the venerable Bunsen burner, its classical configuration adapted with precision to modulate fuel and air flows, thereby engendering a stable laminar flame conducive to speed measurements⁹. Concurrently, specialized tubes, typically fashioned from quartz or glass, afford a controlled environment wherein laminar flame speed can be meticulously observed and quantified¹⁰.

A conceptual departure takes place with the introduction of spherical vessels, enabling the examination of flame characteristics within confined spatial parameters. This entails the observation of the radial expansion resulting from a centrally ignited spark, affording insights into the measurement of laminar flame speed¹¹. Schlieren imaging, an optical technique, makes an entrance, wherein alterations in refractive index are harnessed to visually depict flame front structures, facilitating the quantification of laminar flame speed with a sophisticated degree of precision⁹.

The analytical purview extends to pressure-time analysis, a methodological cohort engaged in the monitoring of pressure fluctuations during combustion¹². By scrutinizing pressure-time curves, researchers discern nuanced patterns, facilitating the inference of laminar flame speed and a deeper comprehension of the combustion process. Concomitantly, Particle Image Velocimetry (PIV)⁹

introduces a dynamic facet, utilizing seeded particles and laser technology to meticulously track their movement, elucidating flow velocities and, by extension, laminar flame speed¹².

The Bunsen burner, a laboratory mainstay, serves as the experimental apparatus. In this method, the burner is adjusted to produce a stable flame by carefully controlling the flow rates of both the fuel and the oxidizer (usually air)^{6, 9, 11}. The resulting flame is smooth and non-turbulent, representing the laminar flame. To measure the laminar flame speed, researchers typically set up a combustion chamber with optical access, allowing for observation and recording of the flame front. The flame is then ignited at the center of the chamber, and its propagation is monitored over time. The key variables include the distance traveled by the flame and the corresponding time elapsed ^{13, 14}. By analyzing this data, scientists can calculate the laminar flame speed—essentially, the rate at which the flame front advances through the mixture⁴. The Bunsen method offers simplicity and reliability, making it an enduring choice in combustion research.

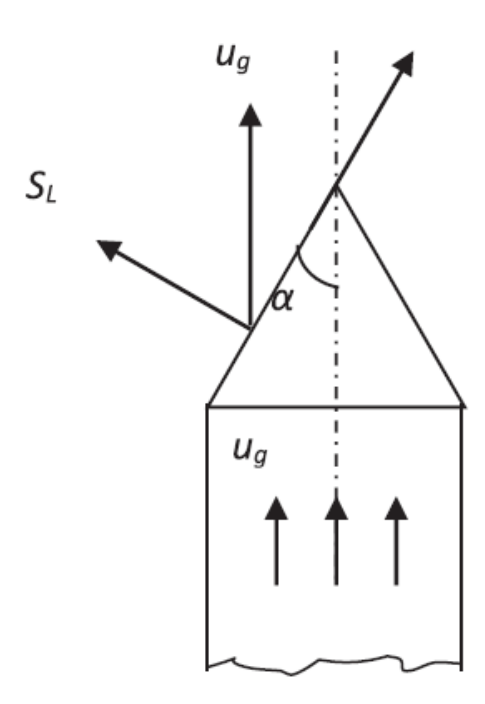


Fig. 1. Illustration depicting the burner method in laminar conditions⁹.

Its controlled conditions allow for precise measurements, and the setup is adaptable to different experimental requirements. Moreover, the Bunsen burners ubiquity in laboratory settings ensures accessibility for researchers across various disciplines. Fig. 1 shows the diagram of the front of a Bunsen burner which is used for calculating S_L values.

Equivalence ratios and laminar flame speeds are intricately linked in the realm of combustion, providing valuable insights into the efficiency and characteristics of fuel-air mixtures. Equivalence ratio, denoted by φ , expresses the ratio of the actual fuel-air mixture to the stoichiometric mixture required for complete combustion. A stoichiometric mixture is represented by φ =1, while values less than 1 indicate fuel-rich conditions and values greater than 1 signify fuel-lean conditions.

Laminar flame speed, on the other hand, represents the speed at which a laminar flame front advances through a combustible mixture under specific conditions. It is influenced by factors such as fuel composition, temperature, and pressure. The relationship between equivalence ratios and laminar flame speeds is complex. In fuel-rich mixtures (ϕ <1), the excess fuel can enhance flame stability, leading to higher laminar flame speeds. Conversely, fuel-lean mixtures (ϕ >1) may exhibit lower laminar flame speeds due to limited fuel availability hindering the combustion process.

This project focuses on identifying laminar flame speeds at various equivalence ratios for different fuel-air mixtures. As said earlier, it will employ numerical models to calculate flame speeds at various ratios, temperatures and pressures and compare them with that from experiments.

3. RESULTS AND DISCUSSION

3.1 Impact of equivalence ratio on laminar flame speeds of various fuel and air mixtures.

3.1.1 Methane-air mixtures

The experimental results obtained for methane—air mixtures at various equivalence ratios were analyzed. Fig. 2 shows the comparison of the present measurements of laminar burning velocity for methane/air and with literature experimental data^{3, 4, 15}.

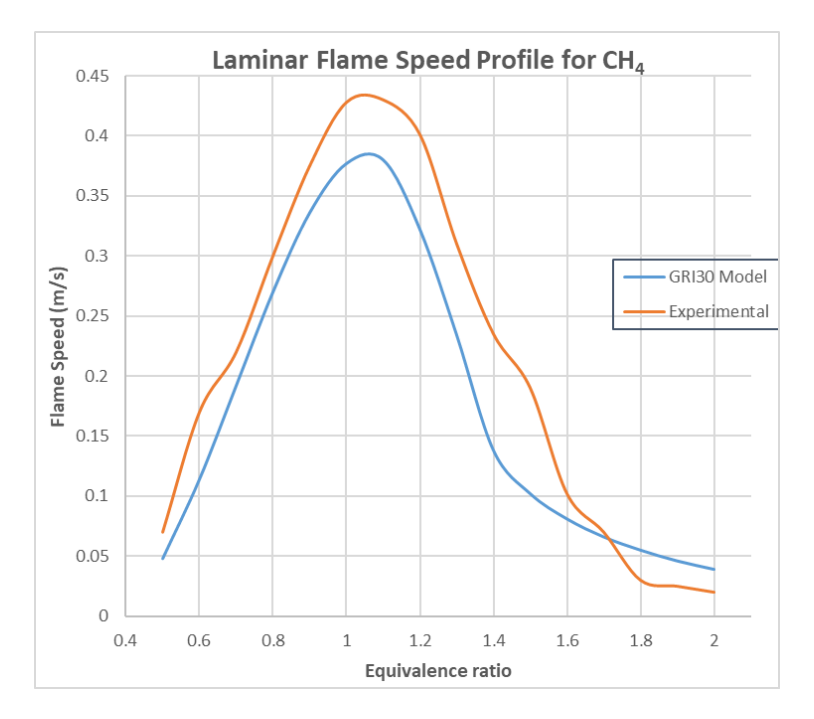


Fig. 2. Comparison of the methane-air mixture laminar flame speeds at 298 K, and 1 atm with the reported work in literature^{3, 15}.

The composition of air is 0.21 mol fraction O_2 and 0.79 mol fraction N_2 . The measured flame speeds are in good agreement with each other and the literature values. For these measurements, the 2σ combined uncertainty is typically below ± 0.05 m/s for the flame speeds. The maximum flame speed is approached at an equivalence ratio of 1.1, which is slightly higher than the stoichiometric mixture. The same is true for the experimental result as well. In general, the GRI30 mechanism undershoots the experimental result.

3.1.2 Hydrogen-air mixtures

Fig. 3 shows the comparison of the present numerical measurements of laminar flame speed for hydrogen/air mixtures with experimental data from Aung, et al. ¹⁶ and Kuznetsov, et al. ¹⁴. The theoretical flame speeds for this fuel mixture are estimated from the H2O2 model which is built-in the Cantera library.

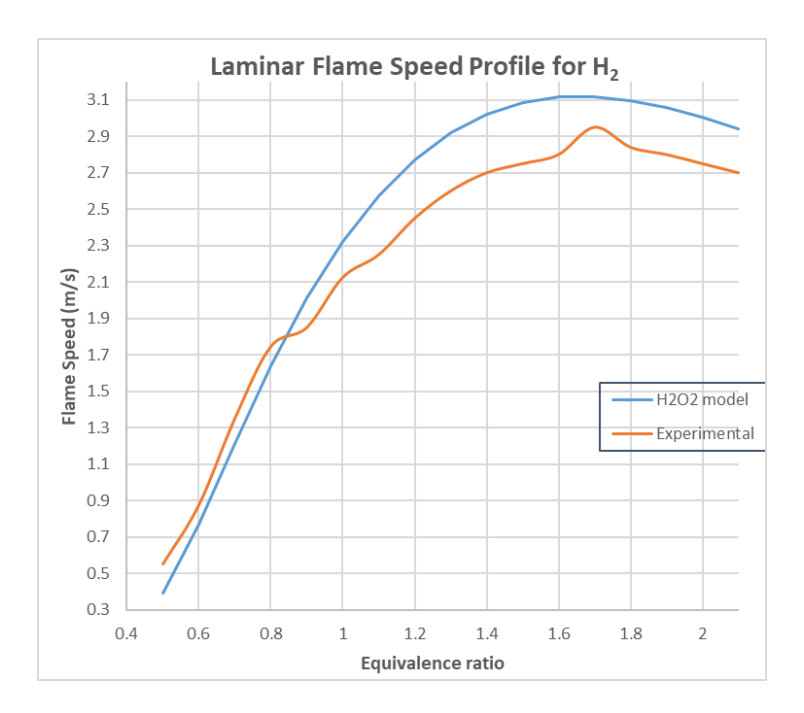


Fig. 3. Comparison of the hydrogen-air mixture laminar flame speeds at 298 K, and 1 atm with the reported work^{13, 14} in literature.

The maximum flame speed is approached at an equivalence ratio of 1.7, which is almost twice as high as the stoichiometric mixture. The same is true for the experimental result as well. In general, the H₂O₂ model mechanism overshoots the actual experimental result, especially at high ratios. The reason behind the disparity in very rich mixtures is not clearly understood. It could be attributed, in part, to the limitation in accurately approximating the flame radius linearly, possibly due to the optical window's small size. Despite this, it is important to highlight that the positive Markstein length for rich mixtures suggests that the unstretched laminar propagation speed should

surpass the window dimensions. Additionally, if the corresponding Markstein length is known, adjustments can be made to the medium-sized laminar burning velocities determined from the pressure–time history.

3.1.3 Ethane-air mixtures

Fig. 4 shows the experimental⁴ and computed flame speeds of ethane/air mixtures. The measured unstretched laminar flame speeds increase with increasing equivalence ratios, and the peak value shifts to the stoichiometric mixture side.

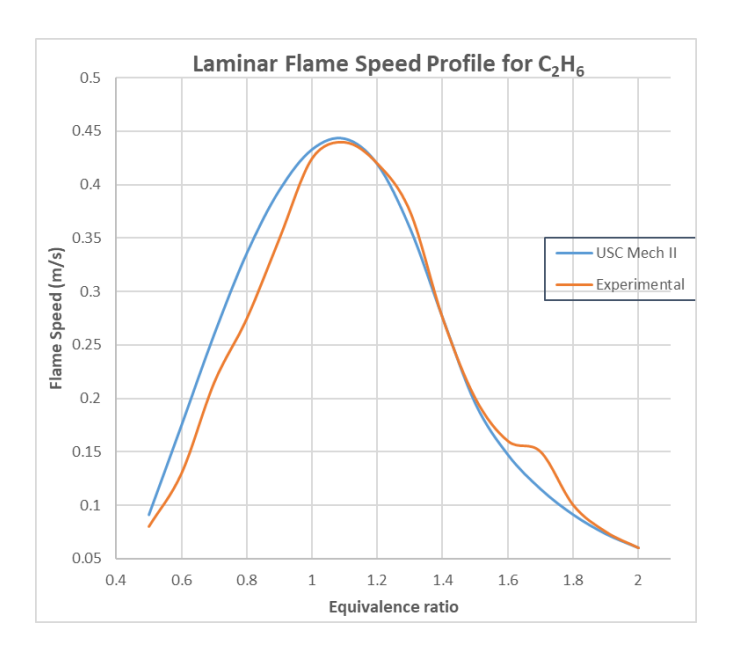


Fig. 4. Comparison of the ethane-air mixture laminar flame speeds at 298 K, and 1 atm with the reported work⁴ in literature.

USC Mech II results in over-prediction of the data by an average of 4 cm/s for equivalence ratios that are lower than 1.1. Beyond this value, in general, the model is in excellent agreement with that of the experimental results. The peak of C₂H₆/air mixture flames occurs at the equivalence ratio of 1.1. This ratio also corresponds to the location of the maximum adiabatic flame temperature, T_{ad}. The observed over-predictions in USC Mech II ethane/air flames are attributed to potential inaccuracies in the ethyl radical reaction kinetics. An avenue for enhancement involves substituting the rate constants of two reactions associated with the ethyl radical in USC Mech II

with values reported elsewhere⁷. This adjustment holds promise for improving the accuracy in predicting S_Ls and extinction strain rates for ethane/air flames.

3.1.4 Ethylene-air mixtures

Fig. 5 shows the experimental and computed flame speeds of ethylene/air mixtures. The measured unstretched laminar flame speeds increase with increasing equivalence ratios.

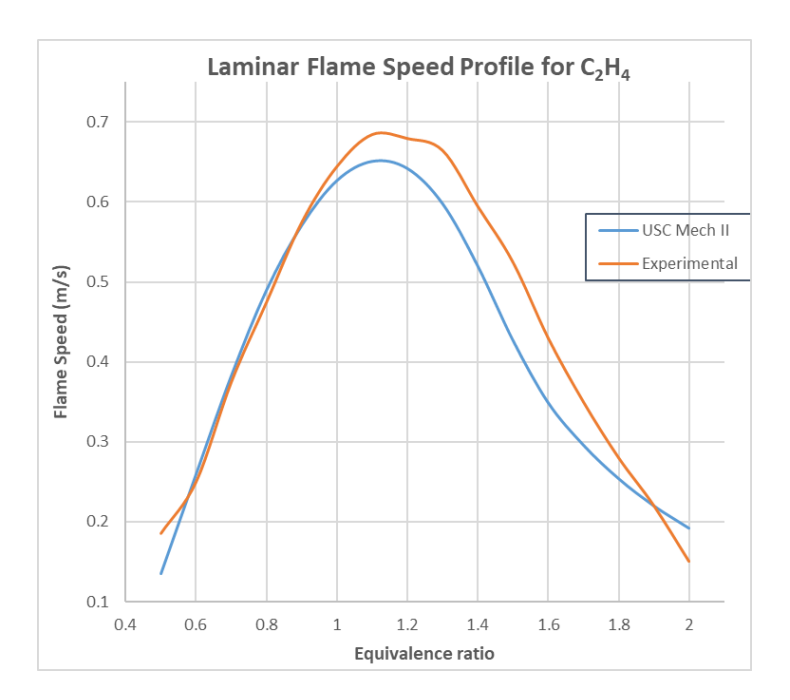


Fig. 5. Comparison of the ethylene-air mixture laminar flame speeds at 298 K, and 1 atm with the reported work^{15, 17} in literature.

The peak value shifts to the stoichiometric mixture side, which is predicted as with more fuel supply, the flame propagates at high speeds. The peak of C₂H₄/air mixture flames occurs at the equivalence ratio of 1.1. The maximum flame speed reached around this point is about 0.64-0.67 m/s. In summary, USC Mech II agrees well with the experimental data at atmospheric pressure. It is seen that, on the fuel-lean side, all the values collapse quite well. At stoichiometric and the fuel-rich side, notable discrepancies are found among the previous data, which could be due to the different extrapolation models.

3.1.5 Propane-air mixtures

Propane finds widespread applications, including laboratory investigations into oxidation processes and utilization in internal combustion engines. In contrast to simpler structured hydrocarbon fuels like methane and ethane, the thermochemical and combustion characteristics of propane closely resemble those of more intricate practical fuels⁴. Fig. 6 shows the experimental and computed flame speeds of propane/air mixtures. The measured unstretched laminar flame speeds increase with increasing equivalence ratios, and the peak value shifts to the stoichiometric mixture side. The values obtained were compared with reported results from literature. The present results overshoot the experimental predictions from lean to the stoichiometric mixtures, while they match well for rich mixture conditions. The current results match well with the literature data for the entire mixture range at 1 atm within the uncertainty limits.

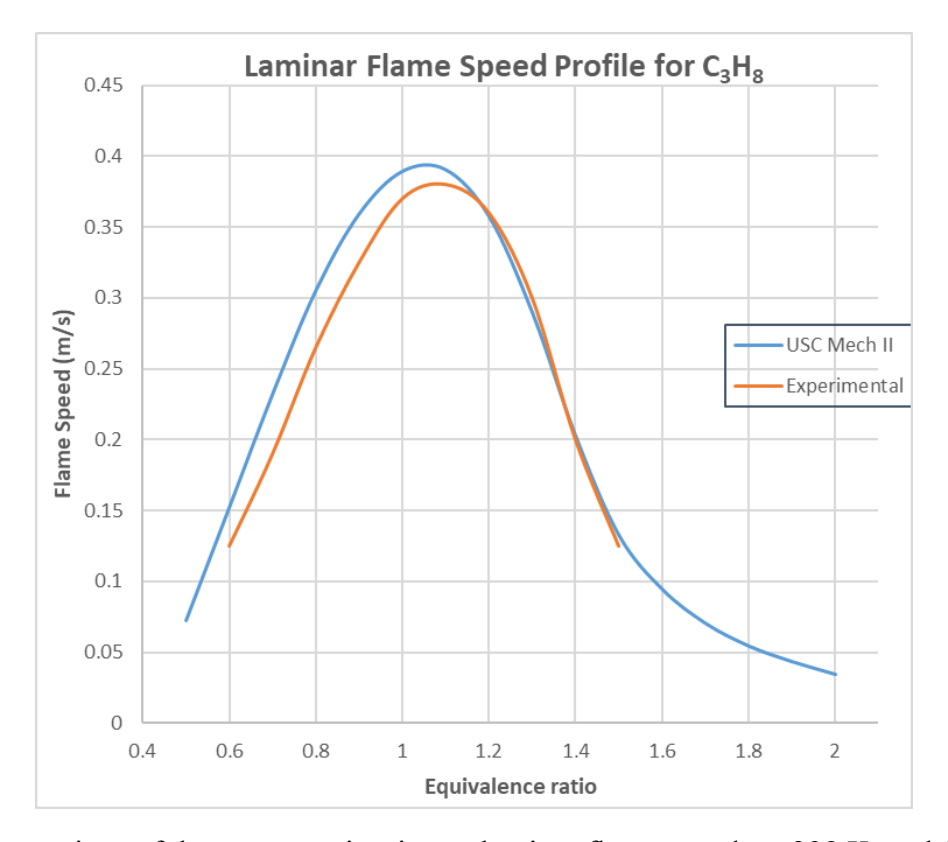


Fig. 6. Comparison of the propane-air mixture laminar flame speeds at 298 K, and 1 atm with the reported work¹⁷ in literature.

3.2 Flame speed calculations near LFL range

Based on the above graphs, it is now clear that the models now decently predict the experimental results. However, as the focus of this project is to test the model accuracy at the LFL range, it is vital to compare the flame speeds of different models with that of the experimental results at the lower equivalence ratios.

Table 1 shows the comparison of laminar flame speed values at lean stoichiometric ratios. Five gases are compared at equivalence ratios ranging from 0.5 to 0.7. For CH₄, there is considerable discrepancy between the experimental and the theoretical value at a ratio of 0.5 and 0.6, and this difference narrows down as the ratio rises to 0.7. A similar trend is seen in H₂ as well. As noted earlier, the H2O2 model predicts quite accurately when it comes to estimating flame speeds near stoichiometric ratios. Furthermore, for ethane, the values show no proper trend as the error in values stays around 20% for all the lower ratios. This might be likely due to the model inaccurately predicting the yields of certain elementary reactions that occur during the combustion of ethane. Moving on, the USC Mech II model seems to predict quite reasonably well for Ethylene, particularly at the equivalence ratios of 0.6 and 0.7. It shows that the reactions that break down the double bond in Ethylene go as predicted by the kinetic model. Finally, errors again propagate around 20% for propane as well. This must be attributed to the way alkanes behave when they undergo combustion. Firstly, as the chain length increases, more activation energy is required to break the C-H bonds. For instance, methane bonds require much less energy to breakdown compared to ethane and propane. Thus, I believe, using the same model and kinetic mechanisms for higher alkanes will be problematic as the activation energies differ for breaking the same C-H bond for higher alkanes. That's why Propane's discrepancy is higher to that of Ethane, which itself has high deviation rate compared to Methane.

Table 2 shows the LFL values of typical flammable gases and their corresponding flame speeds. It also predicts the LFL values of 15 different flammable gases by solving for the composition of the fuel-air mixture at which the flame speed is zero. Fsolve function is utilized to solve for the composition in Python. Additionally, the deviation column refers to the difference between the US or UK standard LFL values and the one predicted by a particular model. For instance, for methane, the US standard LFL value is 5% vol in air. However, the model predicts that this value be lower at 4.325 and thus this gives rise to a deviation of around 15% between these values. These deviations represent the percentage difference between the LFL values predicted by the model and the LFL values obtained from experimental data. In general, larger deviations indicate a greater discrepancy between the model predictions and experimental observations. The materials exhibiting the highest deviations in Lower Flammable Limit (LFL) values between the USC Mech II model (US) and experimental values (EN) are ethane, ammonia, n-butane, and benzene. These substantial discrepancies can be attributed to the intricate combustion chemistry of these substances, where the model may struggle to accurately capture the complex reaction pathways and conditions near the LFL. Ethane and n-butane involve extensive networks of reactions, contributing to notable deviations. Additionally, benzene's unique combustion characteristics pose challenges for accurate modeling. It is also important to note that kinetic models are difficult to generate as they involve inherent complexity of combustion processes, necessary simplifications for computational efficiency, limited validation data, challenges in capturing temperature and pressure dependencies, uncertainties in kinetic data, and the potential neglect of crucial transport phenomena.

3.3 Concentrations of fuel-air mixtures at set S_L values

The model-predicted flame speeds were used to draw a graph of these flame speeds against the LFL value itself. Fig. 7 shows this correlation of the model-predicted flame speeds against the US Standard LFL values. Notably, a general trend emerges, indicating an inverse relationship between LFL values and flame speeds. Materials with higher LFL values tend to exhibit lower flame speeds, while those with lower LFL values often have higher flame speeds. This trend aligns with the intuitive expectation that substances requiring higher concentrations for combustion (higher LFL values) might combust more slowly. Additionally, outliers like ammonia, with a considerably high LFL value but a relatively high flame speed, underscore the complexity of combustion behaviors that go beyond a simple inverse correlation. Methane, for instance, stands out as an outlier with a relatively high LFL value of 5 but a notably low flame speed of 0.049. This divergence could be attributed to the intricate combustion kinetics of methane, showcasing the importance of considering individual material characteristics beyond a generalized trend.

Finally, in Table 3, compositions of each fuel-air mixture were computed, again by using the Fsolve model, but by setting the flame speed to 2 cm/s and 4 cm/s, respectively. In the table, the deviation columns represent the difference between the composition values at the LFL and the ones calculated at 2 cm/s and 4 cm/s, accordingly. Analyzing the deviations at 2 cm/s and 4 cm/s provides valuable insights into the combustion characteristics of the flammable gases. At 2 cm/s, several gases exhibit significant deviations from their flame speeds at the Lower Flammable Limit (LFL). For gases like methane, ethane, and propane, the deviations at 2 cm/s are relatively moderate, suggesting a reasonable agreement between model predictions and experimental concentrations. However, at 4 cm/s, there is a notable reduction in deviations for most gases. This

decrease in deviation at higher speeds could be attributed to the increased kinetic energy and more efficient mixing at elevated velocities, influencing the combustion process.

Ammonia and acetylene, despite having substantial deviations at both velocities, showcase a trend where the deviation at 4 cm/s is comparatively lower than at 2 cm/s. This observation suggests that these gases might exhibit more predictable combustion behaviors at higher flow velocities, potentially due to enhanced turbulence effects and improved mixing, resulting in closer agreement between model predictions and experimental concentrations. In summary, the deviations at 2 cm/s highlight variations between predicted and experimental concentrations at lower flow velocities, while the reduced deviations at 4 cm/s suggest a trend towards improved agreement, possibly influenced by enhanced mixing and laminar effects at higher speeds.

To conclude, it is safe to take a minimum flame speed of 4 cm/s as a common speed for all gases. The deviations at 4 cm/s are less than 15% for most gases, except possibly Acetylene, which for some reason exhibits a strange and unique combustion behavior compared to other gases.

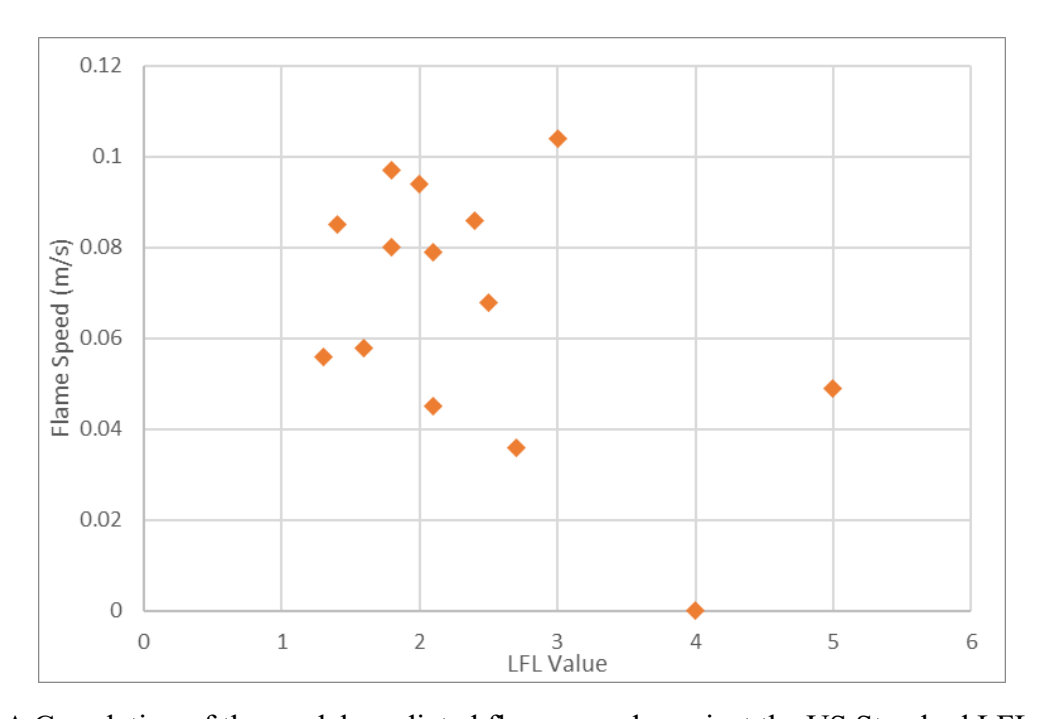


Fig. 7. A Correlation of the model-predicted flame speeds against the US Standard LFL values.

Table 1. Comparison of flame speed values near the lower LFL range for hydrocarbon flammable gases at 298 K and 1 atm.

Flammable gas	Equivalence ratio	Experimental flame speed (in m/s)	Model-predicted flame speed (in m/s)	Deviation (in %)	Reference(s)
	0.5	0.06	0.048	20.0	
Methane (CH ₄)	0.6	0.17	0.114	24.0	18
(- ')	0.7	0.22	0.192	12.7	
	0.5	0.55	0.393	24.4	
Hydrogen (H2)	0.6	0.875	0.772	2 11.8	
(====)	0.7	1.35	1.212	10.2	
	0.5	0.08	0.091	13.7	
Ethane (C ₂ H ₆)	0.6	0.15	0.175	16.7	17, 20, 21
(=====)	0.7	0.215	0.26	20.9	
	0.5	0.165	0.135	18.2	
Ethylene (C ₂ H ₄)	0.6	0.25	0.26	4.0	22
(02114)	0.7	0.375	0.383	2.13	
	0.5	0.060	0.072	20.0	
Propane (C ₃ H ₈)	0.6	0.125	0.152	21.6	23
(55220)	0.7	0.19	0.232	22.1	

Table 2. LFL values of typical flammable gases and their corresponding flame speeds.

Flammable gas	LFL value (vol% in air)	Equivalence Ratio	Moles (Basis: 100 mol)	Model used	Flame Speed at US LFL (m/s)	Model predicted LFL value (vol% in air)	Deviation (in %)	Ref(s)
Methane	US: 5 EN: 4.4	US: 0.501 EN: 0.485	CH ₄ : 5.000 O ₂ : 19.958 N ₂ : 75.042	GRI30 Mech III	0.049	4.235	US: 15.3 EN: 3.75	15, 19
Hydrogen	US: 4 EN: 4	US: 0.198 EN: 0.198	H ₂ : 4.000 O ₂ : 20.168 N ₂ : 75.832	H2O2	0.000	4.000	US: 0.0 EN: 0.0	14, 16, 24
Ethane	US: 3 EN: 2.5	US: 0.551 EN: 0.543	C ₂ H ₆ : 3.000 O ₂ : 20.168 N ₂ : 75.832	USC Mech II	0.104	2.150	US: 28.3 EN: 14.0	15, 17
Ethylene	US: 2.7 EN: 2.3	US: 0.405 EN: 0.385	C ₂ H ₄ : 2.700 O ₂ : 20.441 N ₂ : 76.859	USC Mech II	0.036	2.365	US: 12.4 EN: 2.83	15, 17
Propane	US: 2.1 EN: 1.7	US: 0.513 EN: 0.482	C ₃ H ₈ : 2.100 O ₂ : 20.567 N ₂ : 77.333	USC Mech II	0.079	1.750	US: 16.7 EN: 2.94	15, 17
Propylene	US: 2.4 EN: 2.0	US: 0.558 EN: 0.536	C ₃ H ₆ : 2.400 O ₂ : 20.504 N ₂ : 77.096	USC Mech II	0.086	2.103	US: 13.7 EN: 2.94	15
Isobutane	US: 1.8 EN: 1.3	US: 0.551 EN: 0.543	C ₄ H ₁₀ : 1.800 O ₂ : 20.630 N ₂ : 77.570	UCSD 2016	0.097	1.492	US: 12.2 EN: 2.94	15

Isopentane	US: 1.4 EN: 1.3	US: 0.405 EN: 0.385	C ₅ H ₁₂ : 1.400 O ₂ : 20.714 N ₂ : 77.886	NUI-PI- Modify mech	0.085	1.750	US: 16.7 EN: 2.94	25
Ammonia	US: 15 EN: 15.4	US: 0.513 EN: 0.482	NH ₃ : 15.000 O ₂ : 17.857 N ₂ : 67.143	USC Mech II	0.102	2.103	US: 28.3 EN: 14.0	6
1,3-Butadiene	US: 2 EN: 1.4	US: 0.558 EN: 0.536	C ₄ H ₆ : 2 O ₂ : 20.588 N ₂ : 77.412	USC Mech II	0.094	1.492	US: 12.4 EN: 2.83	15
1-Butene	US: 1.6 EN: 1.4	US: 0.551 EN: 0.543	C ₄ H ₈ : 1.600 O ₂ : 20.672 N ₂ : 77.728	USC Mech II	0.058	1.221	US: 16.7 EN: 2.94	22
n-Butane	US: 1.8 EN: 1.4	US: 0.405 EN: 0.385	C ₄ H ₈ : 1.800 O ₂ : 20.630 N ₂ : 77.570	RTRC Mech III	0.080	1.750	US: 28.3 EN: 14.0	15, 20
Propyne	US: 2.1 EN: 1.9	US: 0.513 EN: 0.482	C ₃ H ₄ : 2.100 O ₂ : 20.567 N ₂ : 77.333	RTRC Mech III	0.045	2.103	US: 28.3 EN: 14.0	19
Acetylene	US: 2.5 EN: 2.3	US: 0.558 EN: 0.536	C ₂ H ₂ : 2.500 O ₂ : 20.504 N ₂ : 77.333	RTRC Mech III	0.068	1.492	US: 12.4 EN: 2.83	15
Benzene	US: 1.3 EN: 1.2	US: 0.558 EN: 0.536	C ₆ H ₆ : 1.300 O ₂ : 20.735 N ₂ : 77.965	RTRC Mech III	0.056	1.232	US: 16.7 EN: 2.94	26

Table 3. Concentrations of flammable gases when the laminar flame speed is 0.02 and 0.04 m/s.

Flammable	LFL	Flame speed	Concentration	Deviation at	Concentration	Deviation
gas	value	at LFL	at 2 cm/s	2 cm/s (%)	at 4 cm/s	at 4 cm/s
			(vol% in air)		(vol% in air)	(%)
Methane	5	0.049	4.622	7.563	5.095	1.89
Hydrogen	4	0	-	-	-	-
Ethane	3	0.104	2.341	21.97	2.581	13.97
Ethylene	2.7	0.036	2.871	6.34	2.591	4.04
Propane	2.1	0.079	1.744	16.97	1.891	9.96
Propylene	2.4	0.086	1.821	24.14	2.031	15.38
Isobutane	1.8	0.075	1.374	23.69	1.519	15.61
Isopentane	1.4	0.085	1.243	16.53	1.321	10.02
Ammonia	15	0.102	12.232	21.21	13.543	12.20
1,3- Butadiene	2	0.094	1.451	27.43	1.642	17.88
1-Butene	1.6	0.089	1.401	12.47	1.523	4.81
n-Butane	1.8	0.095	1.293	28.18	1.454	19.20
Propyne	2.1	0.052	1.943	7.46	2.101	0.04
Acetylene	2.5	0.023	3.277	31.09	3.445	37.82
Benzene	1.3	0.098	1.092	15.97	1.148	11.66

4. CONCLUSION

To conclude, I have successfully correlated the laminar flame speed with the lower flammability limit from some of the commonly employed fuel-air mixtures. Firstly, laminar flame speed profiles were generated by gathering data points over a range of equivalence ratios both from literature and from the numerical models which had kinetic, thermodynamic and transport data in it. The numerical models that were executed by Cantera in Python predicted closely with the experimental data. In general, the graphs showed a similar trend of increasing flame speeds with fuel-air mixture concentrations before reaching a peak value at around φ = 1.1 and then drop back at rich fuel mixtures, except for hydrogen which has a pack value at φ = 1.7 or 1.8. Secondly, near the LFL range, the S_L values tend to be more than 85% accurate, at all ratios, when compared with the experimental results. Moreover, at the LFL value itself, S_L values were calculated and almost all

of them were close to zero, as predicted. Hydrogen had an exact value of 0 m/s at the LFL while most other gases reached a closer to this value with a 0.01 precision. Back calculating the fuel-air mixture composition at 0 cm/s gave model-predicted LFL values which were less than 20% deviated from the standard ones. Finally, from the correlation graph, it was clear that most gases had higher than 4 cm/s flame speed, so to confirm this, the mixture composition is again calculated at 4 cm/s flame speed and all the values were less than 15% deviated from the experimental LFL value. Thus, it is safe to assume that the minimum flame speed for all gases be at 4 cm/s.

5. FUTURE STEPS

This capstone project shed some light on elucidating the variations in laminar flame speeds at a variety of equivalence ratios for significant single-component fuels. A comprehensive examination reveals a need for substantial efforts to establish a consistent database of laminar flame speed values, facilitating the accurate modelling and verification of reaction mechanism models. Several recommendations emerge from this scrutiny:

A unified methodology is essential for stretch correction derived from raw data obtained through both the spherical and stagnation flame methods. The provision of raw experimental data for analysis by other research groups is vital for comparative analysis. Transparent reporting of initial operating conditions, gas/oxidizer purity and composition, instrumentation accuracy, and uncertainty calculations is pivotal for meaningful cross-method comparisons²⁶.

Limited data exists for mixture temperatures surpassing 500 K. The diverging channel method is the sole approach directly measuring laminar flame speed at elevated temperatures²⁵. An in-depth examination of measurements using various methods can provide more accurate assessments of the temperature exponent, 'a,' enabling the refinement of precise reaction mechanism models at elevated temperatures. Meager measurements are available under high-pressure conditions. Recent

efforts with the heat-flux method have yielded accurate trends in pressure exponent, 'b,' and its comparison with kinetic model predictions for methane fuel, albeit limited to 5 atm pressure 13. The constant volume method holds promise for obtaining measurements at higher pressures and temperatures pertinent to gas turbines and internal combustion engines 9. The focus should be on refining techniques for laminar flame speed measurement under these conditions and comparing data across different measurement methods to bolster the development of enhanced kinetic models. The inherent flame instability when using air as the oxidizer and the challenges in extrapolating results using helium gas make this task particularly demanding.

The application of developed single-component fuel kinetic models to intricate hydrogen-enriched and multi-component surrogate fuels, applicable in real engineering systems, is imperative¹³. Concurrently measuring laminar propagation speeds under elevated mixture temperatures and pressures is crucial for enhancing system design. Increased emphasis is needed to enhance the closed vessel bomb hot wire method, demonstrating potential for measuring laminar flame speeds both at high pressures and temperatures.

6. REFERENCES

Format: Accounts of Chemical Research

- (1) Akram, M.; Kumar, S. Measurement of laminar burning velocity of liquified petrolium gas air mixtures at elevated temperatures. *Energy & fuels* **2012**, *26* (6), 3267-3274.
- (2) Xie, Y.; Li, Q. A review on mixing laws of laminar flame speed and their applications on H2/CH4/CO/air mixtures. *International Journal of Hydrogen Energy* **2020**, *45* (39), 20482-20490.
- (3) Ranzi, E.; Frassoldati, A.; Grana, R.; Cuoci, A.; Faravelli, T.; Kelley, A. P.; Law, C. K. Hierarchical and comparative kinetic modeling of laminar flame speeds of hydrocarbon and oxygenated fuels. *Progress in Energy and Combustion Science* **2012**, *38* (4), 468-501.
- (4) Amirante, R.; Distaso, E.; Tamburrano, P.; Reitz, R. D. Laminar flame speed correlations for methane, ethane, propane and their mixtures, and natural gas and gasoline for spark-ignition engine simulations. *International Journal of Engine Research* **2017**, *18* (9), 951-970.
- (5) Akram, M.; Kishore, V. R.; Kumar, S. Laminar burning velocity of propane/CO2/N2-air mixtures at elevated temperatures. *Energy & Fuels* **2012**, *26* (9), 5509-5518.
- (6) Hayakawa, A.; Goto, T.; Mimoto, R.; Arakawa, Y.; Kudo, T.; Kobayashi, H. Laminar burning velocity and Markstein length of ammonia/air premixed flames at various pressures. *Fuel* **2015**, *159*, 98-106.
- (7) Katoch, A.; Millán-Merino, A.; Kumar, S. Measurement of laminar burning velocity of ethanolair mixtures at elevated temperatures. *Fuel* **2018**, *231*, 37-44.
- (8) Lapalme, D.; Seers, P. Influence of CO2, CH4, and initial temperature on H2/CO laminar flame speed. *International Journal of Hydrogen Energy* **2014**, *39* (7), 3477-3486.
- (9) Mascarenhas, V. J.; Weber, C. N.; Westmoreland, P. R. Estimating flammability limits through predicting non-adiabatic laminar flame properties. *Proceedings of the Combustion Institute* **2021**, *38* (3), 4673-4681.
- (10) Lhuillier, C.; Brequigny, P.; Lamoureux, N.; Contino, F.; Mounaïm-Rousselle, C. Experimental investigation on laminar burning velocities of ammonia/hydrogen/air mixtures at elevated temperatures. *Fuel* **2020**, *263*, 116653.
- (11) Monteiro, E.; Bellenoue, M.; Sotton, J.; Moreira, N. A.; Malheiro, S. Laminar burning velocities and Markstein numbers of syngas—air mixtures. *Fuel* **2010**, *89* (8), 1985-1991.
- (12) Shu, T.; Xue, Y.; Zhou, Z.; Ren, Z. An experimental study of laminar ammonia/methane/air premixed flames using expanding spherical flames. *Fuel* **2021**, *290*, 120003.
- (13) Han, W.; Dai, P.; Gou, X.; Chen, Z. A review of laminar flame speeds of hydrogen and syngas measured from propagating spherical flames. *Applications in Energy and Combustion Science* **2020**, *1*, 100008.

- (14) Kuznetsov, M.; Kobelt, S.; Grune, J.; Jordan, T. Flammability limits and laminar flame speed of hydrogen—air mixtures at sub-atmospheric pressures. *International journal of hydrogen energy* **2012**, *37* (22), 17580-17588.
- (15) Davis, S.; Law, C. K. Determination of and fuel structure effects on laminar flame speeds of C1 to C8 hydrocarbons. *Combustion Science and Technology* **1998**, *140* (1-6), 427-449.
- (16) Aung, K.; Hassan, M.; Faeth, G. Flame stretch interactions of laminar premixed hydrogen/air flames at normal temperature and pressure. *Combustion and flame* **1997**, *109* (1-2), 1-24.
- (17) Jomaas, G.; Zheng, X.; Zhu, D.; Law, C. K. Experimental determination of counterflow ignition temperatures and laminar flame speeds of C2–C3 hydrocarbons at atmospheric and elevated pressures. *Proceedings of the Combustion Institute* **2005**, *30* (1), 193-200.
- (18) Wu, Y.; Modica, V.; Rossow, B.; Grisch, F. Effects of pressure and preheating temperature on the laminar flame speed of methane/air and acetone/air mixtures. *Fuel* **2016**, *185*, 577-588. Egolfopoulos, F. N.; Cho, P.; Law, C. K. Laminar flame speeds of methane-air mixtures under reduced and elevated pressures. *Combustion and flame* **1989**, *76* (3-4), 375-391.
- (19) Hermanns, R.; Konnov, A.; Bastiaans, R.; De Goey, L.; Lucka, K.; Köhne, H. Effects of temperature and composition on the laminar burning velocity of CH4+ H2+ O2+ N2 flames. *Fuel* **2010**, *89* (1), 114-121.
- (20) Mitu, M.; Razus, D.; Giurcan, V.; Oancea, D. Experimental and numerical study of laminar burning velocity of ethane—air mixtures of variable initial composition, temperature and pressure. *Energy & fuels* **2014**, *28* (3), 2179-2188.
- (21) Giurcan, V.; Razus, D.; Mitu, M.; Oancea, D. Numerical study of the laminar flame propagation in ethane-air mixtures. *Central European Journal of Chemistry* **2014**, *12*, 391-402.
- (22) Kim, H. J.; Van, K.; Lee, D. K.; Yoo, C. S.; Park, J.; Chung, S. H. Laminar flame speed, Markstein length, and cellular instability for spherically propagating methane/ethylene—air premixed flames. *Combustion and Flame* **2020**, *214*, 464-474.
- (23) Wang, Z.; Yelishala, S. C.; Yu, G.; Metghalchi, H.; Levendis, Y. A. Effects of carbon dioxide on laminar burning speed and flame instability of methane/air and propane/air mixtures: a literature review. *Energy & Fuels* **2019**, *33* (10), 9403-9418.
- (24) Tse, S. D.; Zhu, D.; Law, C. K. Morphology and burning rates of expanding spherical flames in H2/O2/inert mixtures up to 60 atmospheres. *Proceedings of the combustion institute* **2000**, *28* (2), 1793-1800.
- (25) Konnov, A. A.; Mohammad, A.; Kishore, V. R.; Kim, N. I.; Prathap, C.; Kumar, S. A comprehensive review of measurements and data analysis of laminar burning velocities for various fuel+ air mixtures. *Progress in Energy and Combustion Science* **2018**, *68*, 197-267.

(26) Wang, G.; Li, Y.; Yuan, W.; Zhou, Z.; Wang, Y.; Wang, Z. Investigation on laminar burning velocities of benzene, toluene and ethylbenzene up to 20 atm. *Combustion and Flame* **2017**, *184*, 312-323.

7. APPENDIX

7.1 Flame Code function for calculating S_L

def compute_SL(mechName, T, P, X, thickness=False, loglevel=1,
plot=True):

""" Compute laminar flame speed of the homogeneous mixture

Parameters

mechName: name of input mechanism file (xml or cti-format)

T: temperature in [K]

P: pressure in [Pa]

X: dictionary of mixture composition

thickness: calculate flame thickness? default is False

loglevel: log level (0-8); default is 1

Returns

SL: laminar flame speed in [m/s]

theta L: laminar flame thickness in [m] if thickness is True

.....

import cantera as ct

import numpy as np

import matplotlib.pyplot as plt

```
## define gas
if isinstance(mechName, str) and mechName.endswith('cti'):
            = ct.Solution(infile=mechName)
    gas
else:
    gas
           = mechName
gas.TPX = T, P, X
## set up free flame object
width = 0.03
       = ct.FreeFlame(gas, width=width)
f.transport_model = 'Mix'
f.flame.set_steady_tolerances(default=[1.0e-5, 1.0e-13])
f.flame.set_transient_tolerances(default=[1.0e-4, 1.0e-13])
f.set refine criteria(ratio=3, slope=0.06, curve=0.12)
f.set max jac age(10, 10)
# set the sequence of time steps to try when Newton fails
f.set time step(1e-5, [2, 5, 10, 20, 40])
## solve with energy disabled first
print('Disabling energy ...')
f.energy_enabled = False
f.solve(loglevel, refine_grid=False)
## laminar flame speed
try:
    print('Enabling energy ...')
    f.energy enabled = True
    f.solve(loglevel, refine grid=True)
    SL = f.velocity[0]
```

```
dTdz = np.gradient(f.T)/np.gradient(f.grid)
        theta_L = (max(f.T) - min(f.T))/max(dTdz)
    except ct.CanteraError:
        SL = 0
        theta L = 0
    if plot:
        fig,ax = plt.subplots()
        ax.plot(f.grid*1000, f.T-273.15, '-x')
        ax.set(xlabel='grid [mm]', ylabel='T [C]')
    if not thickness:
        return SL
    else:
        return SL, theta L
7.2 Code for returning S<sub>L</sub> value at a particular T, P and X
import cantera as ct
import matplotlib.pyplot as plt
from compute SL import compute SL
if __name__ == "__main__":
    # mechanism name (using built-in Gri-MECH 3.0)
    gas = ct.Solution('mech.yaml')
    # T in {K}
    T = 298
```

```
# P in {Pa]
P = 101325

# X
X = {'C4H612': 0.43, '02': 5.5, 'N2': 5.5*3.76}

# compute lamianr flame speeds - SL
SL = compute_SL(gas, T, P, X)
print(f'laminar flame speed is {SL:.3f} m/s')
```